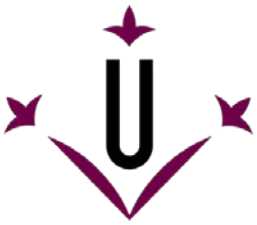

Universitat de Lleida

Document downloaded from:

http://hdl.handle.net/10459.1/48749

The final publication is available at:

http://dx.doi.org/10.1016/j.foodhyd.2015.01.032

Copyright

cc-by-nc-nd, (c) Elsevier, 2015


Està subjecte a una llicència de Reconeixement-NoComercial-SenseObraDerivada 4.0 de Creative Commons

Edible films from essential-oil-loaded nanoemulsions: physicochemical characterization and antimicrobial properties

Alejandra Acevedo-Fani
Laura Salvia-Trujillo
María Alejandra Rojas-Graü
Olga Martín-Belloso*
* Author to whom correspondence should be addressed: omartin@tecal.udl.es

Department of Food Technology
University of Lleida - Agrotecnio Center
Av. Alcalde Rovira Roure 191
25198, Lleida, Spain

ABSTRACT

Edible films including active ingredients can be used as an alternative to preserve food products. Essential oils (EOs) exhibit antimicrobial activity against pathogenic microorganisms but their low water solubility limits the application in foods. To improve water dispersion and protect EOs from degradation, nano-sized emulsions emerge as a viable alternative. Nanoemulsions containing EOs and polysaccharides could be used to form edible films with functional properties. This study was focused on the evaluation of physical, mechanical and antimicrobial properties of alginate-based edible films formed from nanoemulsions of EOs. Nanoemulsions containing thyme (TH-EO), lemongrass (LG-EO) or sage (SG-EO) oil as dispersed phase and sodium alginate solution as continuous phase were prepared. The average droplet size of nanoemulsions was reduced after the microfluidization treatment exhibiting multimodal size distributions. The ζ-potentials of nanoemulsions were between -41 mV and -70 mV depending on the type of EO used. The lowest whiteness index was found in SG-EO nanoemulsions, whereas those containing TH-EO showed the highest value. Films formed from SG-EO nanoemulsions exhibited higher transparency, water vapor resistance and flexibility than films formed from TH-EO or LG-EO. Edible films containing TH-EO were those with the strongest antimicrobial effect against inoculated *Escherichia coli*, achieving up to 4.71 Log reductions after 12 hours. Results obtained in the present work evidence the suitability of using nanoemulsions with active ingredients for the formation of edible films, with different physical and functional properties.

Keywords

Nanoemulsions, microfluidization, essential oils, edible films, antimicrobial activity, sodium alginate

1 INTRODUCTION

Edible films have been proposed as an alternative of food packaging to improve the quality and safety of food products. This technology protects foods from dehydration and acts as gases barrier with the surrounding media. In addition, edible films may serve as carriers of active compounds such as antimicrobials, antioxidants and texture enhancers, among others. Sodium alginate is a polysaccharide isolated from marine brown algae, widely used in the food industry as thickening agent, which also has film-forming properties (Krochta, Baldwin, & Nisperos-Carriedo, 1994). Essential oils (EOs) are aromatic oily liquids extracted from plant materials and commonly utilized as flavoring in foodstuffs (Burt, 2004). Their antimicrobial properties against several pathogenic microorganisms involved in foodborne illness have been demonstrated in previous investigations (Alboofetileh, Rezaei, Hosseini, & Abdollahi, 2014; Oriani, Molina, Chiumarelli, Pastore, & Hubinger, 2014). For this reason, the scientific community and food industry are considering the use of EOs as potential preservatives of natural origin. Nevertheless, their incorporation in food systems is mainly limited by flavor considerations, since effective antimicrobial doses may exceed organoleptic acceptance levels (Lambert, Skandamis, Coote, & Nychas, 2001). In addition, EOs have low-water solubility, meaning their dispersion within aqueous-based products is rather difficult.

Nanoemulsions are being increasingly used to encapsulate, protect and deliver lipophilic ingredients to liquid foods or minimally processed fruits and vegetables (Bhargava, Conti, da Rocha, & Zhang, 2015; Donsì, Cuomo, Marchese, & Ferrari, 2014; Kim, Ha, Choi, & Ko, 2014). Literature refer nanoemulsions as emulsions with very small droplet size, below 100 nm (McClements, 2011; Solans, Izquierdo, Nolla, Azemar, & Garcia-Celma, 2005). The small particle size in nanoemulsions has two important consequences: i) the possibility of enhancing physicochemical properties and stability; and ii) the ability of improving

biological activity of lipophilic compounds by increasing the surface area per unit of mass (McClements & Rao, 2011). This fact also allows using lower doses of active ingredients. Recent studies have shown an enhancement of the physical properties of EOs-loaded nanoemulsions regarding to their equivalent conventional emulsions (Salvia-Trujillo, Rojas-Graü, Soliva-Fortuny, & Martín-Belloso, 2013). In addition, it has been also observed a higher antibacterial activity in nanoemulsions containing EOs (Buranasuksombat, Kwon, Turner, & Bhandari, 2011; Liang et al., 2012; Severino et al., 2015).

In this sense, nanoemulsions based on polysaccharides such as alginate and EOs as antimicrobial agents may be used for edible films formation, which could be considered a new generation of edible packaging. The particular properties observed in nanoemulsions regarding to the conventional emulsions could be extrapolated to the physicochemical and functional properties of the edible films formed from them. Previous studies have evaluated the formation of films based on nanoemulsions prepared by low-energy methods and high-energy techniques such as ultrasounds or high-speed homogenization (Bilbao-Sáinz, Avena-Bustillos, Wood, Williams, & McHugh, 2010; Otoni, Pontes, Medeiros, & Soares, 2014; Otoni, Moura, et al., 2014). However, up to our knowledge, systematic studies have not been reported about the properties of polysaccharide-based films made from EOs-loaded nanoemulsions prepared by microfluidization. Therefore, the purpose of this study was to evaluate the antimicrobial, physical and mechanical properties of edible films obtained from alginate-based nanoemulsions loaded with EOs (Thyme, TH-EO; lemongrass, LG-EO or sage, SG-EO), as well as characterizing the physicochemical properties of the EO nanoemulsions relating them with the edible film properties.

2 MATERIALS AND METHODS

Food grade sodium alginate was supplied by FMC Biopolymers Ltd (Scotland, UK). Nonionic surfactant (Tween 80) was purchased from Scharlau (Spain), and plasticizer (glycerol) was provided by Fisher Scientific (UK). Thyme (TH-EO; *Thymus vulgaris*), lemongrass (LG-EO; *Cymbopogon citratus*) and sage (SG-EO; *Salvia officinalis*) essential oils were purchased from Essential arôms (Spain).

2.1 PREPARATION OF FILM FORMING NANOEMULSIONS (FFN)

Sodium alginate dispersions were prepared by dissolving 3% w/v in double distilled water at 70°C. A coarse emulsion was obtained by mixing alginate dispersions at room temperature, glycerol (2% v/v), Tween 80 (3% v/v) and TH-EO, LG-EO or SG-EO (1% v/v) in a high-speed blender at 17500 rpm for 2 minutes (Ultra-turrax, Jake & Kunkel, Staufen, Germany). To prepare nanoemulsions, coarse emulsions were pumped into the microfluidizer (M110P, Microfluidics, Massachusetts, USA) at 150 MPa for three cycles. Temperature of nanoemulsions during processing was maintained below 15ºC with an external coiling coil immersed in an ice-water bath and placed at the exit of the interaction chamber. All samples were prepared using ultra-pure water obtained from a Milli-Q filtration system. Alginate films (ALG) were also made without the addition of EO (alginate 3% w/v, Tween 80 3% v/v and glycerol 2 % v/v) to be considered as control.

2.2 CHARACTERIZATION OF FILM-FORMING NANOEMULSIONS (FFN)

2.2.1 PARTICLE SIZE AND ζ-POTENTIAL

Particle size, polidispersity index and ζ-potential were analyzed with a Zetasizer Nano ZS laser diffractometer (Malvern Instruments Ltd, Worcestershire, UK). Particle size was measured by dynamic light scattering (DLS) at 633 nm, 25 ºC and using a backscatter detector of 173 º. Film-forming nanoemulsions (FFN) were first diluted with ultra-pure water

to 1:20 to avoid multiple scattering effects. The average droplet size (z-average) and polidispersity index were reported. Polidispersity index (PDI) value is a measure of heterogeneity in the droplets size distribution. PDI values close to 0 indicate homogeneous size distributions, whereas PDI values close to 1 indicate heterogeneous size distributions. The surface charge at the interface of oil droplets within FFN (ζ-potential) was measured by phase-analysis light scattering (PALS).

2.2.2 WHITENESS INDEX AND VISCOSITY

The color of the FFN was determined with a Minolta CR-400 colorimeter (Konica Minolta Sensing, Inc., Osaka, Japan), using an illuminant D_{65} and the 10º observer angle. The device was calibrated in a white standard plate (Y = 94, x = 0.3158, y = 0.3222). A crystal flat-faced cuvette was filled with FFN and then placed at the top of the measuring device of the colorimeter. CIE L^*, a^* and b^* values were utilized to calculate whiteness index (WI) throughout equation 1(Vargas, Cháfer, Albors, Chiralt, & González-Martínez, 2008):

$$WI = 100 - \sqrt{(100 - L^*)^2 + \left(a^{*2} + b^{*2}\right)} \quad (1)$$

The viscosity of FFN was measured in aliquots of 10 ml using a vibro-viscosimeter SV-10 (A&D Company, Tokyo, Japan), vibrating at 30 Hz and constant amplitude.

2.3 FILM FORMATION

Nanoemulsions and alginate film-forming solutions were treated with a vacuum pump to remove air bubbles and avoid the presence of micro-holes in film structure. Then, oil-containing and control films were formed by casting in crystal plates of 30 x 40 cm, previously covered with Mylar paper. Films were dried at room temperature for 24 hours and peeled off from Mylar paper for further determinations.

2.4 CHARACTERIZATION OF EDIBLE FILMS

2.4.1 SCANNING ELECTRON MICROSCOPY

Aluminum stubs with films were dried in a heater at 60ºC for 48 h. Films were fixed with carbon and metalized with evaporated gold in a Blazers SCD 050 sputter coater (Balzers Union AG, Liechtenstein) to grant electrical conductive properties. Microstructure of films surface were examined using a Scanning Electron Microscope with an acceleration voltage of 10 kV and a working distance of 10 mm (DSM 940 A, Zeiss, Germany).

2.4.2 COLOR AND OPACITY

Film color and opacity were measured with a colorimeter (CR-400, Konica Minolta Sensing, Inc., Osaka, Japan), using an illuminant D_{65} and the 10º observer angle. The instrument was calibrated with a standard white plate (Y = 94.00, x = 0.3158, y = 0.3222). Measurements were performed by placing film squares of 30 mm x 30 mm onto a white background. Chromaticity coordinates CIE L^*, a^*, b^* were recorded to obtain the color difference (ΔE^*), which was calculated using equation 2 (Pires et al., 2013):

$$\Delta E^* = ((L^* - L_o)^2 + (a^* - a_o)^2 + (b^* - b_o)^2)^{0.5} \quad (2)$$

Where L^*, a^*, b^* are the color coordinates of the films, and L_o, a_o, b_o values are those corresponding to the white background (L_o = 90.97, a_o = 0.08, b_o = -0.28).

Film opacity was obtained by measuring the CIE Y coordinates of edible films (30 mm x 30 mm) onto a white and black background. Opacity was calculated by equation 3 (Pires et al., 2013):

$$Opacity = {}^{Y_b}/_{Y_w} \times 100 \quad (3)$$

Where Y_b is the Y coordinate measured on the black background, and Y_w is the Y coordinate measured on the white background.

2.4.3 FILM THICKNESS

Film thickness was determined with IP 65 micrometer (Mitutoyo Manufacturing, Tokio, Japan). Thickness was taken in five random points of the film.

2.4.4 WATER VAPOR PERMEABILITY

Water vapor permeability (WVP) of films was evaluated gravimetrically at 25ºC using a modified version of ASTM standard method E96-00 (ASTM, 2000). Methylmethacrylate test cups (internal diameter of 3 cm, outer diameter 4.5 cm and depth of 2.0 cm) were used to determine WVP. Cups were filled with distilled water (6 mL) and circular samples of films were placed over the cups and sealed using a cap with a rubber O-ring. The diameter of film exposure was 3 cm. Cups with films were placed in glass containers with hermetic covers containing a saturated solution of magnesium chloride (MgCl2.6H2O), with 33 % of relative humidity at 25 ºC. Cups weights were recorded at 60 min intervals over 6 h.

Weight loss data versus time were analyzed by lineal regression to obtain the slope (m_1) of the curve in g/s. Water vapor transmission rates (WVTR) through the film and WVP were calculated as described in equation 4 and 5 (Chinnan & Park, 1996; Kaya & Kaya, 2000).

$$WVTR = m_1/A \quad (4)$$

$$WVP = L \times WVTR/(\rho_i - \rho_a) \quad (5)$$

Where A (m^2) is the exposed film area, ρ_i (Pa) and ρ_a (Pa) are the vapor pressures of saturated air and air with 33% RH, respectively, at 25ºC. L is the average film thickness (m).

2.4.5 MECHANICAL PROPERTIES

Edible films were evaluated by tensile tests (elongation at break, EAB; and tensile strength, *TS*) and puncture tests (puncture force, *PF*) using a TA-TX2 texture analyzer (Stable Micro Systems, Goldaming, Surrey, UK). TS and EAB were determined by ASTM standard method D882-97 (ASTM, 1991). Rectangular strips (25 mm x 100 mm) were equilibrated into a cabin with a saturated solution of nitrate magnesium ($Mg(NO_3)_2$) (Fisher Scientific, UK) with HR 50 ± 5 % at 25 ºC during 5 days. After equilibration time, strips were placed in self-tightening roller grips and measurements were performed with an initial grip separation of 50 mm, a cross-head speed of 1 mm/s and using a load cell of 5 kg. TS and EAB were calculated by equations 6 and 7:

$$TS = F_{max}/A \quad (6)$$

$$EAB = \left(L/L_o\right) \times 100 \quad (7)$$

Where F_{max} is the maximum load for breaking films (N), A is the cross-sectional area of the sample (thickness x width). L_o represents the initial gage length (50 mm) of the sample, L the final length of the film before the moment of rupture.

Puncture analyses were determined by ASTM D6241-04 standard method (ASTM, 2004). The samples (30 mm x 30 mm) were equilibrated at the same conditions used for tensile tests. Films were placed on a film support ring adjusted to the texture analyzer. An aluminum circular plate with two screws was fitted on the film to avoid slippage. Then, a stainless steel spherical probe of 5 mm diameter scrolled perpendicularly to the film surface at a constant speed of 1 mm/s^{-1} until cross the sample. PF was obtained from the force-displacement curves recorded by Texture Exponent 32 software (Stable Micro Systems, Goldaming, Surrey, UK).

2.4.6 ANTIMICROBIAL ACTIVITY ANALYSIS

2.4.6.1 INOCULUM PREPARATION

A strain of *Escherichia coli* 1107 (Laboratoire de Répression des Fraudes (LRF), Montpellier, France) was provided from the culture collection of the Department of Food Technology of the University of Lleida, Spain. The *E. coli* culture was kept refrigerated at 5ºC in slant tubes with Tryptone Soy Agar (TSA) (Biokar Diagnostics, France). The strain was then grown in Tryptone Soy Broth (TSB) (Biokar Diagnostics, France) at 37ºC for 12 h, to obtain cells in stationary growth phase. The final concentration of the culture was 10^9 UFC.mL^{-1}.

2.4.6.2 ANTIMICROBIAL ACTIVITY

Antimicrobial activity of edible films was determined according to their *E. coli* inactivation with a method described by other authors with some modifications (Kristo, Koutsoumanis, & Biliaderis, 2008; Sánchez-González, Cháfer, Hernández, Chiralt, & González-Martínez, 2011). TSA containing NaCl 3% was used as a model of solid food system (TSA-NaCl) with high pH (∼6.5) and high a_w (∼0.98). Approximately 20 ml of TSA-NaCl medium was poured into petri dishes of 9 cm of diameter, solidified and stored under refrigeration. The *E. coli* culture was diluted to reach a concentration of 10^6 UFC/ml and aliquots of 1 µL were spread on the agar surface and coated with edible film circles of 9 cm diameter. TSA-NaCl plates inoculated and uncoated were used as control. Straightaway, coated and uncoated TSA-NaCl plates were left at room temperature for 12 hours. During the first four hours, antimicrobial activity of TSA-NaCl plates was evaluated hourly. Afterwards, essays were carried out every two hours. For this purpose, 10 g of agar were carefully removed aseptically from Petri dishes and put in sterile stomacher bags with 90 ml of saline peptone (Biokar Diagnostics, France). Bags were homogenized for 2 minutes in a Stomacher blender. Serial dilutions were prepared and spread onto McConkey-Sorbitol Agar (Biokar Diagnostics, France). Plates were incubated at 37ºC for 24 h and after colonies were counted.

2.5 STATISTICAL ANALYSIS

Droplet size, ζ-potential, viscosity and whiteness index of EO-nanoemulsions, as well as color, thickness and WVP parameters of edible films were performed in triplicate. Antimicrobial activity was run in duplicate and mechanical analyses were evaluated in ten samples per type of film. Two repetitions of each type of film were prepared for all the tests. The one-way analysis of variance (ANOVA) was applied to analyze data using the Statgraphics Plus 5.1 software package (Statistical Graphics Co., Rockville, MD, EE.UU). Fisher's least significant difference (LSD) procedure was applied to evaluate differences among average results with a significant level of 95%. Pearson's correlation coefficients were estimated to establish relationships between the physical properties of both nanoemulsions and edible films.

3 RESULTS AND DISCUSSION

3.1 FILM-FORMING NANOEMULSIONS PROPERTIES

3.1.1 DROPLET SIZE AND SIZE DISTRIBUTION

The droplet size of nanoemulsions containing different EOs in sodium alginate solution were measured since they might have a relevant impact on features such as, color, permeability, or mechanical properties of edible films. The corresponding oil droplet size distribution expressed by intensity can be seen in Figure 1. The size distributions were multimodal regardless the EO type, presenting several peaks corresponding to oil droplets of different size. In general, it was observed two major intensity peaks around 20 nm and 190 nm in the droplet size distributions, and a small peak around 6000 nm. The peak at 20 nm could be related to the presence of surfactant micelles that were not adsorbed at the oil-water interface of nanoemulsions, which are typically around 10 nm (Heydenreich, 2003; Rao & McClements, 2012a), or to oil droplets disrupted during the microfluidization process. The

peak around 190 nm corresponded to EOs droplets (Cramer Flores et al., 2011; Liang et al., 2012). Residual intensity peaks close to the detection limit of the equipment (6000 nm) suggested the presence of larger oil droplets that were not disrupted or alginate colloidal structures. Nanoemulsions loaded with SG-EO presented the highest intensity peak at the 20 nm region indicating that most of the droplets had very small diameters after microfluidization. Nanoemulsions containing TH-EO showed the lowest peak at 20 nm, which could be due to the fact that surfactant molecules were mostly adsorbed at the oil-water interface compared to those formed with SG-EO or LG-EO, or the surfactant activity was affected by the presence of alginate molecules and did not adsorbed quickly enough during the formation of nanodroplets, obtaining more droplets in the 190 nm region than in the 20 nm region. It is known that the surface activity of small molecule surfactants is determined by the oil polarity (Dickinson, 2009; Kralova & Sjöblom, 2009; Stang, Karbstein, & Schubert, 1994). TH-EO have shown a relatively high water solubility as it has been reported the need of ripening inhibitors, such as corn oil, in order to change EO polarity, thereby enabling its stabilization in nanoemulsions (Chang, McLandsborough, & McClements, 2012; Rao & McClements, 2012a). Salvia and co-workers (2013) reported narrow size distributions in nanoemulsions made with sodium alginate (1 % w/v) and LG-EO (1 % v/v) treated by microfluidization at the same processing conditions used in this study. Multimodal size distributions obtained in FFN prepared in the present work could be attributed to the high viscosity of the system due to the presence of sodium alginate at 3 % w/v in the continuous phase. The high viscosity of nanoemulsions could affect the efficacy of droplets disruption because the microfluidizer was not able to generate sufficiently intense disruptive forces at the pressure used (Jafari, Assadpoor, He, & Bhandari, 2008). Other authors have attributed the polydisperse behavior of nanoemulsions to the possible presence

of instability phenomena after homogenization due to re-coalescence of oil droplets (Atarés, Bonilla, & Chiralt, 2010).

On the other hand, the average droplet size of nanoemulsions of TH-EO, LG-EO and SG-EO were 82 ± 3 nm, 41 ± 9 nm, 35 ± 7 nm, respectively, showing polydispersity indices ranging from 0.65 to 0.52 (Table 1). In a preliminary study, the droplet size of coarse emulsions was measured presenting average droplet sizes above those obtained in nanoemulsions (TH: 236 ± 30 nm, LG: 591 ± 50 nm, SG: 113 ± 8 nm). The z-average size is a consistent parameter given for monodisperse systems measured by the DLS technique. This value is usually quite near to the peak of the particle size distribution. However, when samples present non-monodisperse distributions, interpretation of the z-average is more complicated and it is necessary to consider the size distributions regarding the mass and number of particles. Particle size measurements by the DLS technique are generated from the analysis of the fluctuations in scattered light intensity where large particles scatter light more strongly than small particles. In this sense, a small population of large droplets could be represented as a big intensity peak, whereas a similar population of small droplets is shown as a smaller intensity peak. Droplet size distributions presented in terms of volume of the particles were analyzed, in order to find relevant effects of peaks observed in the intensity distribution graph on the overall droplet size distribution of nanoemulsions. In all cases, it was found a major peak located below 100 nm, which could confirm that most of the EO droplets within nanoemulsions showed diameters in the nano-range, suggesting that the majority of oil droplets were disrupted by microfluidization.

In addition, the type of EO significantly affected ($p < 0.05$) average droplet size of nanoemulsions (Table 1). Incorporation of TH-EO led to larger droplet sizes than in nanoemulsions containing SG-EO, which suggests different grades of affinity between the oil and the alginate phases as well as the non-ionic surfactant used in the formulation. This

particular effect can be related to the chemical composition of EOs, which is highly variable depending on their biological origin. The presence of surface-active substances in EO composition itself could increase their water solubility. EOs containing surfactant-like compounds may accumulate at the oil-water interface lowering the interfacial tension in emulsions and facilitating the droplet disruption during homogenization. In addition, other important properties such as oil polarity and viscosity can intervene on the resulting droplet size (Edris & Malone, 2012; Ziani, Fang, & McClements, 2012).

3.1.2 ζ-POTENTIAL

The electrical charge of TH-EO, LG-EO and SG-EO droplets in nanoemulsions are shown in Table 1. The ζ-potential values ranged between -41 mV and -70 mV. In general, electrical charge of droplets is governed by the charge of surfactants adsorbed around oil droplets, which can be of anionic, cationic or non-ionic nature. Nanoemulsions prepared in this study contained a non-ionic surfactant (Tween 80); then, one would expect an electrical charge close to zero. However, results showed oil droplets in nanoemulsions presented ζ-potentials highly negative. In this sense, it has been described that the incorporation of ionic biopolymers in the continuous phase of emulsions can change the ζ-potential of oil droplets (Dickinson, 2003). Although, most biopolymers work as thickening agents rather than surfactants in emulsions, they can be partially adsorbed to oil droplets by different types of interactions in certain conditions (Dickinson, 2009). Therefore, the negative electrical charge observed in EOs nanoemulsions stabilized with a non-ionic surfactant can be attributed to the adsorption of sodium alginate molecules dispersed in the continuous phase, due to their anionic nature. Choi and co-workers (2011) previously observed negative electrical charge in multilayer nanoemulsions containing capsaicin and Tween 80 when they incorporated the oil-surfactant phase in alginate solutions. It has been described that electrical charge of droplets plays an important role in nanoemulsions stability. When this charge is sufficiently large,

droplets are prevented from aggregation because of the electrostatic repulsion among them. Droplets with electrical charge above +30 mV or below -30 mV are considered to be stable to within the nanoemulsion system (Heurtault, 2003). Therefore, nanoemulsions formed in the present study could be considered stable by electrostatic mechanisms. Moreover, electrical charge of oil droplets was significantly ($p<0.05$) influenced by the EO type. Nanoemulsions formed with SG-EO showed the largest ζ-potential in comparison with those containing LG-EO and TH-EO, which might be related with to the presence of ionisable groups in EOs composition that lead to different electrostatic interactions among oil, surfactant and biopolymer chains at the interface of the system. According to our results, Bonilla and co-workers (2012) found differences between the ζ-potentials of emulsions containing basil and thyme oil as disperse phase and chitosan in the continuous phase.

3.1.3 WHITENESS INDEX

Whiteness index values (WI) of EOs-loaded nanoemulsions are shown in Table 1. All nanoemulsions presented a visual appearance rather translucent; however, measurements of WI showed slight differences depending on EO type. For instance, SG-EO nanoemulsions presented the lowest WI with 23.53; whereas, LG-EO and TH-EO nanoemulsions showed the highest with 25.38 and 27.95, respectively. It is well known that emulsion appearance is mainly determined by the presence of oil droplets, therefore parameters such as droplet size, concentration and refractive index directly influence the overall emulsions optical properties (Chantrapornchai, Clydesdale, & McClements, 1998). Nanoemulsions are described as slightly turbid systems, which it is attributed to the fact that small droplets scatter light weakly; therefore, as the droplet size increase, the light scattering is strong and emulsions tend to be opaque. In most of the cases, transparency of film-forming solutions is desirable in order to obtain films that scarcely modify the food color. In this study, it was observed that

WI decreased as the droplet size lessened, thereby indicating that optical properties of nanoemulsions were dependent on the particle size of nanoemulsions.

3.1.4 VISCOSITY

Table 1 shows viscosities of nanoemulsions including EOs as disperse phase and sodium alginate as continuous phase. Viscosity is one of the most relevant parameters in emulsions since it has a significant effect on system stability and depends on the rheology of emulsion phases. The viscosity of pure sodium alginate solutions was 800 mPa.s. However, nanoemulsions exhibited significantly lower viscosity values than sodium alginate solutions (Table 1). This behavior may be explained by the effect of microfluidization on biopolymer viscosity, since high-shear forces can induce conformational changes or degradation of polymer chains, changing their molecular weight. Previous authors have confirmed this trend by subjecting several types of biopolymer-based emulsions to high-shear homogenization (Bonilla et al., 2012; Salvia-Trujillo et al., 2013). Moreover, the EO type significantly ($p < 0.05$) affected viscosity of nanoemulsions, being those with LG-EO incorporated the most viscous (616 ± 62 mPa.s). Since EOs are complex mixtures of different components, this might lead to different adsorption kinetics between alginate molecules and oil droplets, thus changing the initial concentration of biopolymer in the continuous phase and thereby, changing the emulsion viscosity (Bonilla et al., 2012).

3.2 EDIBLE FILMS PROPERTIES

3.2.1 MICROSTRUCTURE

Microstructure of edible films based on EOs nanoemulsions was examined to get some insights on nanodroplets organization along the biopolymer matrix, and its possible influence on the film properties. SEM images in Figure 2 correspond to the surface of alginate films (ALG) and those containing TH-EO, LG-EO and SG-EO. Figure 2A shows the film top that

372 was dried against air, whereas figure 2B presents the film surface that was dried facing the
373 support paper. As a general trend, microstructure of films made from nanoemulsions was
374 rougher than ALG films (oil-free). The increase in surface coarseness with the presence of
375 EOs have been previously observed by other authors (Norajit, Kim, & Ryu, 2010; Shojaee-
376 Aliabadi et al., 2014). Sánchez-González and co-workers (2011) attributed this fact to the
377 migration of oil droplets upwards the films and further volatilization during water
378 evaporation, resulting in a holey structure.

379 Moreover, it was observed different grades of roughness in the film side in contact with air
380 according to the EO type (Figure 2A). In the case of LG-EO films, noticeable oil body
381 aggregates were observed suggesting that oil droplets were positioned at the film surface in
382 contact with air during drying. On the other hand, edible films obtained from TH-EO or SG-
383 EO nanoemulsions showed continuous surfaces with small circular protuberances, which
384 indicated a better embedding of nanodroplets inside alginate matrix. It has been reported that
385 films made from small droplet size emulsions have shown smoother surface than those
386 obtained from large droplet size emulsions leading to a better stability of droplets within film
387 structure (Fabra, Pérez-Masiá, Talens, & Chiralt, 2011).

388 In contrast, SEM images in Figure 2B showed all film surfaces in contact to the support were
389 rather uniform and absence of protuberances regardless of EO type, which suggested that
390 alginate molecules were preferentially located near the plastic support during drying process.
391 Generally, emulsion-based films experiment a reorganization of lipophilic and hydrophilic
392 components originating a bilayer fashion structure. In concordance with the images observed
393 in Figure 2A and 2B, films formed in this study evidenced a structural arrangement of
394 alginate molecules and EOs governed by their chemical affinity.

395 ### 3.2.2 COLOR AND OPACITY

The optical properties of edible films can change the overall appearance of food products, affecting the consumer acceptance. Table 2 shows optical properties of alginate films (ALG) and those formed from EO nanoemulsions. The EO type significantly ($p < 0.05$) affected L^*, a^*, b^* parameters and difference of color (ΔE^*) in edible films. Lightness, expressed by coordinate L^* was higher in films based on LG-EO and SG-EO nanoemulsions, whereas ALG films and those including TH-EO showed the lowest values. Coordinate a^*, which negative values indicates a green color, significantly decreased to -0.83 ± 0.05 in films containing TH-EO, whereas the other films remained around -0.40. The coordinate b^*, which positive values refer to yellow color, showed a similar trend where the most positive value (6.9 ± 0.6) was observed in films containing TH-EO, thus indicating that these films had a light greenish-yellowish tone. This could be explained by the presence of phenolic compounds in TH-EO, which might have light adsorption at low wavelength (Jouki, Mortazavi, Yazdi, & Koocheki, 2014). Furthermore, the difference of color (ΔE^*) was higher in edible films with TH-EO (58 ± 9), than in those containing SG-EO and LG-EO (11,9 ± 1.4 and 13 ± 3, respectively). In this particular case, we found a strong positive correlation between droplet size of nanoemulsions and ΔE^* values of the matching films, with $r = 0.9424$ (table 4). This means that ΔE^* of edible films was mainly influenced by the droplet size of their film-forming nanoemulsions, and difference of color decreased as the droplet size decreased. We also have found strong relationship between ΔE^* of films and whiteness index of nanoemulsions ($r = 0.9128$). These two correlations let us stablish the robust effect of the optical properties of nanoemulsions on the color characteristics of films made from them.

Opacity of films was significantly different ($p < 0.05$) depending on EO type. Edible films based on LG-EO nanoemulsions showed the highest value (9.7 ± 1.9) compared with ALG films and those made of TH-EO and SG-EO nanoemulsions. This behavior could be explained by the differences in surface roughness observed in the films (figure 3A). LG-EO

421 films presented a coarse surface caused by the presence of oil droplets that moved upwards
422 the film in the drying process, which in turn, could have increased light scattering and led to
423 higher opacity values. On the contrary, films made from TH-EO and SG-EO presented
424 homogeneous surfaces due to a better entrapment of oil droplets within structure, and
425 therefore, light scattering could have diminished.

426 Furthermore, it was observed a positive relationship between ζ-potential of nanoemulsions
427 and opacity of films, with a correlation coefficient of 0.7008 (table 4). In other words, opacity
428 of films decreased as the electrical charge of nanoemulsions was more negative. Probably,
429 the reason of this fact may be linked to the structural conformation of biopolymer chains
430 regarding with their electrical charge; when biopolymers are strongly charged, chains should
431 remain more extended. On the other hand, when the electrical charge is weak biopolymer
432 chains tends to form globular structures, since inter-chain electrical repulsion is partially
433 avoided. In both cases, the resulting film structure and hence, opacity should be fairly
434 different.

435 3.2.3 WATER VAPOR PERMEABILITY AND FILM THICKNESS

436 Water vapor permeability (WVP) measures the diffusion of water molecules through the
437 cross-section of the film and can give an estimation of its barrier property. To prevent or
438 reduce the dehydration of foods, films used as packaging or coatings must control the
439 moisture transport from the product to the environment, hence WVP of edible films should be
440 as low as possible (Ma, Chang, & Yu, 2008). The transference of water vapor is carried out
441 by the hydrophilic fraction of the film and permeability depends on its hydrophilic-lipophilic
442 ratio (Hernandez, 1994). Therefore, the presence of lipid compounds in film structure
443 enhances water barrier properties due to an increased tortuosity that creates a resistance to the
444 water vapor through the film. It has been described that tortuosity is higher when oil phase

445 ratio increases or oil particle size is reduced (Pérez-Gago & Krochta, 2001).
446 EOs are known to decrease WVP of polysaccharide-based films due to their hydrophobic
447 behavior. However, little differences were observed between ALG films and EO-containing
448 films; probably due to the low oil content used in this study. Only films with SG-EO showed
449 a significant reduction compared with ALG films ($p < 0.05$). It is possible this small
450 difference on WVP of films could have been favored by the small droplet size of the
451 equivalent nanoemulsions, leading to a greater distribution of the oil phase in the film
452 structure.

453 On the other hand, films cast from pure alginate solutions had a thickness of 50 ± 3 µm (table
454 3). It was observed films made from LG-EO and SG-EO nanoemulsions presented a
455 significantly smaller thickness ($p < 0.05$). These results could be linked to the droplet size
456 achieved in the film-forming nanoemulsions. Sánchez-González et al., (2011) found a
457 thickness reduction in edible films made from emulsions with small droplet size. They
458 attributed this effect to possible losses of oil phase during film formation, which could
459 decrease the total amount of solids concentration in the film matrix. Furthermore, film
460 thickness exhibited a significant relationship with droplet size of nanoemulsions with a
461 correlation coefficient of 0.6919 (table 4), supporting the dependence of this variables.

462 ### 3.2.4 MECHANICAL PROPERTIES

463 The most common parameters that describes the mechanical properties of edible films are
464 tensile strength (TS) and elongation at break (EAB), which are strongly related to the
465 chemical structure of films (Dufresne & Vignon, 1998). TS indicates the resistance to tension
466 forces and EAB is related to film stretching capacity. The mechanical properties of alginate-
467 based films are shown in Figure 3. Films made from EO nanoemulsions were as resistant as
468 alginate films (ALG) without significant differences ($p < 0.05$) in TS values (Figure 3B).

Although several reports have mentioned that oil addition to film formulation tends to weaken the film by decreasing cohesion forces within the structure (Han & Gennadios, 2005; Zúñiga, Skurtys, Osorio, Aguilera, & Pedreschi, 2012), in this study we obtained nanoemulsion-based films rather resistant, probably due to the low oil content incorporated.

On the other hand, edible films prepared from SG-EO nanoemulsions were the most stretchable (EAB: 78 ± 5 %), whereas films containing LG-EO and TH-EO (EAB: 32 ± 9 % and 41 ± 12 %, respectively) did not show significant differences ($p < 0.05$) regarding ALG films (38 ± 7 %) (Figure 3A). These variations in film flexibility could be partially explained by the influence of the electrical charge of nanoemulsions in the film structure. The repulsive forces among molecules of the same charge can increase the distance between polymers, resulting in a plasticizing effect in the case of charged polymeric film structure (Han & Gennadios, 2005). In this sense, the pronounced difference between electrical charge of SG-EO nanoemulsions (-70 mV) and TH-EO or LG-EO nanoemulsions (-44 mV and -41 mV, respectively) could have led to different grades of flexibility in edible films. In concordance, we observed a strong negative association between ζ-potentials of nanoemulsions and EAB of films, with a correlation coefficient of -0.8527 (table 4). On the other hand, small droplet sizes also may influence film elasticity. As the surface area of oil droplets is larger in film structure, the biopolymer network become more heterogeneous thus decreasing chain-chain interactions and increasing the plasticizing effect. In concordance with this, we found a moderate correlation between droplet size of nanoemulsions and EAB of edible films (r = 0.5383; table 4).

Figure 3B shows the puncture force (PF) of alginate films formed from EOs-loaded nanoemulsions. Puncture resistance is the maximum force required to cause the film break by a penetrating tip and describes film rigidity. Films made from nanoemulsions presented

493 significantly lower values of PF compared with ALG films (11.47 ± 1.05 N). LG-EO films
494 showed the lowest PF (8.58 ± 1.09 N) and the highest value was observed in TH-EO films
495 (9.8 ± 0.5 N). The drop of PF values in films obtained from nanoemulsions could be related
496 to the microfluidization effect on the molecular chains of alginate, which could decrease film
497 rigidity. It has been described high pressure homogenization can affect molecular weight of
498 biopolymers by changing their conformation, thereby, inducing an irreversible ordered-
499 disordered conformation transition and molecular degradation (Lagoueyte & Paquin, 1998).
500 This trend was also reported in biopolymer-based edible films treated by microfluidization
501 (Jiménez, Fabra, Talens, & Chiralt, 2012; Vargas, Perdones, Chiralt, Cháfer, & González-
502 Martínez, 2011).

503 ### 3.2.5 ANTIMICROBIAL ACTIVITY

504 The inhibitory effect against *Escherichia coli* of alginate films (ALG) and those prepared
505 with EOs nanoemulsions is presented in Figure 4. ALG films did not show any antimicrobial
506 activity and the microorganism growth was similar to the TSA-NaCl plates without any film
507 (CT). In line with these results, Pranoto and co-workers (2005) found that alginate films were
508 not able to reduce the *E. coli* growth in 'in-vitro' tests. On the other hand, the type of EO
509 significantly affected antibacterial activity of edible films. In the case of films formed from
510 TH-EO nanoemulsions, the inhibitory effect was significantly strong whereas LG-EO and
511 SG-EO films did not show any growth reduction. In the case of TH-EO films, a dramatic
512 decrease of bacteria population up to 3.97 log reductions during the first contact hour was
513 observed. Moreover, antibacterial effect was prolonged during the contact time between
514 bacteria and antimicrobial films, reaching 4.71 log reductions after 12 hours. The strong
515 inhibitory effect observed in TH-EO films is attributed to the presence of thymol molecules,
516 which is the major compound in TH-EO. Thymol molecules can bind to membrane proteins
517 of microbial cells by hydrophobic interactions, thus changing the membrane permeability.

518 Moreover, thymol is able to disintegrate the outer membrane of gram-negative bacteria,
519 hence releasing lipopolysaccharides and increasing the permeability of cytoplasmic
520 membrane (Juven, Kanner, Schved, & Weisslowicz, 1994; Ultee, Bennik, & Moezelaar,
521 2002). The effectiveness of EOs is also influenced by the sensibility of the microorganism to
522 EO. In this regard, *Escherichia coli* has been described as a sensitive bacteria to the action of
523 TH-EO alone or incorporated in edible film (Emiroğlu, Yemiş, Coşkun, & Candoğan, 2010;
524 Jouki et al., 2014).

525 In contrast, films based on SG-EO nanoemulsions presented less than 1 log reduction of *E.*
526 *coli* population during the first two hours and microbial counts gradually increased until the
527 end of experiments (12 h) (figure 4). This trend suggested a resistance mechanism of the
528 microorganism to SG-EO as the time of exposure was longer. This results are in agreement
529 with others reported previously, where the inhibitory effect of pure SG-EO was low in gram-
530 negative bacteria such as *E.coli* (Gutierrez, Rodriguez, Barry-Ryan, & Bourke, 2008; Shirazi
531 et al., 2008). Similarly, edible films including LG-EO did not show any effect against the *E.*
532 *coli* growth along the contact time studied. Other authors have observed great antibacterial
533 effect of LG-EO edible films against *E.coli* growth (Maizura, Fazilah, Norziah, & Karim,
534 2007; Rojas-Graü et al., 2007). Nevertheless, the absence of antimicrobial effect in LG-EO
535 films found in this study could be partially attributed to volatilization of oil compounds
536 during the film formation. We postulate LG-EO droplets migrated upwards during film
537 drying due to the low density of their antimicrobial compounds (Citral: 0.856 kg/cm^3;
538 limonene: 0.834 kg/m^3 (Rao & McClements, 2012b)). We could support the above mentioned
539 assumption by examining the film microstructure, where surface of LG-EO films in contact
540 with air exhibited a grainy appearance. This means that oil droplets were concentrated on the
541 top of the film (Figure 2A) and could evaporate faster due to the increase vapor pressure of
542 nanometer size droplets (Nuchuchua et al., 2009). However, there are other crucial factors

543 that could affect effectiveness of EOs, such as antagonistic interactions with other ingredients
544 (e.g. proteins or carbohydrates), or the pH of the system (Pires et al., 2013; Raybaudi-
545 Massilia, Mosqueda-Melgar, & Martin-Belloso, 2008).

546 4 CONCLUSIONS

547 The results obtained in the present study give some insights on the relevant effect of
548 preparing edible films using nanoemulsions of EOs as film-forming dispersions. It was found
549 that the most important factors of nanoemulsions affecting the physical properties of edible
550 films were the droplet size and the electrical charge of oil droplets. A decrease on the droplet
551 size and magnitude of the ζ-potential led to relevant changes in the barrier, color and
552 mechanical properties of films. On the other hand, these parameters were not relevant in term
553 of antimicrobial properties of edible films. Rather, the composition of EOs and the
554 susceptibility of the bacteria to those compounds determined the efficacy of films against the
555 microbial growth. Therefore, this work confirms the feasibility of preparing nanoemulsions to
556 enhance encapsulation of EOs and to obtain functional edible films, which might be useful to
557 protect and preserve food products.

558 5 ACKNOWLEDGMENTS

559 This research was supported by the Ministerio de Ciencia e Innovación (Spain) throughout
560 projects ALG2009-11475 and ALG2012-35635. Author Acevedo-Fani also thanks to the
561 University of Lleida for the pre-doctoral grant. Author Martín-Belloso acknowledges to the
562 Institució Catalana de Recerca I Estudis Avançats (ICREA) for the Academia 2008 Award.

6 REFERENCES

ASTM. (1991). Standard test methods for tensile properties of thin plastic sheeting, method D 882-91.Philadelphia, PA: American Society for Testing Materials.

ASTM. (2000). Standard test methods for water vapor transmission of materials, method E 96-00.Philadelphia, PA: American Society for Testing Materials.

ASTM. (2004). Test method for the static puncture strength of geotextiles and geotextile-related products using a 50-mm probe, method D 6241-04. Philadelphia, PA: American Society for Testing Materials.

Alboofetileh, M., Rezaei, M., Hosseini, H., & Abdollahi, M. (2014). Antimicrobial activity of alginate/clay nanocomposite films enriched with essential oils against three common foodborne pathogens. *Food Control*, *36*(1), 1–7.

Atarés, L., Bonilla, J., & Chiralt, A. (2010). Characterization of sodium caseinate-based edible films incorporated with cinnamon or ginger essential oils. *Journal of Food Engineering*, *100*(4), 678–687.

Bhargava, K., Conti, D. S., da Rocha, S. R. P., & Zhang, Y. (2015). Application of an oregano oil nanoemulsion to the control of foodborne bacteria on fresh lettuce. *Food Microbiology*, *47*, 69–73.

Bilbao-Sáinz, C., Avena-Bustillos, R. J., Wood, D. F., Williams, T. G., & McHugh, T. H. (2010). Nanoemulsions prepared by a low-energy emulsification method applied to edible films. *Journal of Agricultural and Food Chemistry*, *58*(22), 11932–8.

Bonilla, J., Atarés, L., Vargas, M., & Chiralt, A. (2012). Effect of essential oils and homogenization conditions on properties of chitosan-based films. *Food Hydrocolloids*, *26*(1), 9–16.

Buranasuksombat, U., Kwon, Y. J., Turner, M., & Bhandari, B. (2011). Influence of emulsion droplet size on antimicrobial properties. *Food Science and Biotechnology*, *20*(3), 793–800.

Burt, S. (2004). Essential oils: Their antibacterial properties and potential applications in foods - A review. *International Journal of Food Microbiology*, *94*(3), 223–253.

Chang, Y., McLandsborough, L., & McClements, D. J. (2012). Physical properties and antimicrobial efficacy of thyme oil nanoemulsions: influence of ripening inhibitors. *Journal of Agricultural and Food Chemistry*, *60*(48), 12056–63.

Chantrapornchai, W., Clydesdale, F., & McClements, D. J. (1998). Influence of Droplet Size and Concentration on the Color of Oil-in-Water Emulsions. *Journal of Agricultural and Food Chemistry*, *46*, 2914–2920.

Chinnan, M. S., & Park, H. J. (1996). Effect of plasticizer level and temperature on water vapor transmission of cellulose-based edible films. *Journal of Food Process Engineering*, *18*(4), 417–429.

Choi, A.-J., Kim, C.-J., Cho, Y.-J., Hwang, J.-K., & Kim, C.-T. (2011). Characterization of Capsaicin-Loaded Nanoemulsions Stabilized with Alginate and Chitosan by Self-assembly. *Food and Bioprocess Technology*, *4*(6), 1119–1126.

Cramer Flores, F., Fagundes Ribeiro, R., Ferreira Ourique, A., Bueno Rolim, C. M., De Bona Da Silva, C., Raffin Pohlmann, A., Stanisçuaski Guterres, S. (2011). Nanostructured systems containing an essential oil: protection against volatilization. *Química Nova*, *34*(6), 968–972.

Dickinson, E. (2003). Hydrocolloids at interfaces and the influence on the properties of dispersed systems. *Food Hydrocolloids*, *17*(1), 25–39.

Dickinson, E. (2009). Hydrocolloids as emulsifiers and emulsion stabilizers. *Food Hydrocolloids*, *23*(6), 1473–1482.

Donsì, F., Cuomo, A., Marchese, E., & Ferrari, G. (2014). Infusion of essential oils for food stabilization: Unraveling the role of nanoemulsion-based delivery systems on mass transfer and antimicrobial activity. *Innovative Food Science & Emerging Technologies*, *22*, 212–220.

Dufresne, A., & Vignon, M. R. (1998). Improvement of starch film performances using cellulose microfibrils. *Macromolecules*, *31*(8), 2693–2696.

Edris, A. E., & Malone, C. F. R. (2012). Preferential solubilization behaviours and stability of some phenolic-bearing essential oils formulated in different microemulsion systems. *International Journal of Cosmetic Science*, *34*(5), 441–450.

Emiroğlu, Z. K., Yemiş, G. P., Coşkun, B. K., & Candoğan, K. (2010). Antimicrobial activity of soy edible films incorporated with thyme and oregano essential oils on fresh ground beef patties. *Meat Science*, *86*(2), 283–8.

Fabra, M. J., Pérez-Masiá, R., Talens, P., & Chiralt, A. (2011). Influence of the homogenization conditions and lipid self-association on properties of sodium caseinate based films containing oleic and stearic acids. *Food Hydrocolloids*, *25*(5), 1112–1121.

Gutierrez, J., Rodriguez, G., Barry-Ryan, C., & Bourke, P. (2008). Efficacy of plant essential oils against foodborne pathogens and spoilage bacteria associated with ready-to-eat vegetables: Antimicrobial and sensory screening. *Journal of Food Protection*, *71*(9), 1846–1854.

Hammer, K. A., Carson, C. F., & Riley, T. V. (1999). Antimicrobial activity of essential oils and other plant extracts. *Journal of Applied Microbiology*, *86*(6), 985–990.

Han, J., & Gennadios, A. (2005). Edible films and coatings: a review. In *Innovations in Food Packaging* (pp. 239–262). Elsevier.

Helander, I. M., Alakomi, H.-L., Latva-Kala, K., Mattila-Sandholm, T., Pol, I., Smid, E. J., Von Wright, A. (1998). Characterization of the Action of Selected Essential Oil Components on Gram-Negative Bacteria. *Journal of Agricultural and Food Chemistry*, *46*(9), 3590–3595.

Hernandez, R. J. (1994). Effect of water vapor on the transport properties of oxygen through polyamide packaging materials. *Journal of Food Engineering*, *22*(1-4), 495–507.

Heurtault, B. (2003). Physico-chemical stability of colloidal lipid particles. *Biomaterials*, *24*(23), 4283–4300.

Heydenreich, A. (2003). Preparation and purification of cationic solid lipid nanospheres—effects on particle size, physical stability and cell toxicity. *International Journal of Pharmaceutics*, *254*(1), 83–87.

Jafari, S. M., Assadpoor, E., He, Y., & Bhandari, B. (2008). Re-coalescence of emulsion droplets during high-energy emulsification. *Food Hydrocolloids*, *22*(7), 1191–1202.

Jiménez, A., Fabra, M. J., Talens, P., & Chiralt, A. (2012). Influence of hydroxypropylmethylcellulose addition and homogenization conditions on properties and ageing of corn starch based films. *Carbohydrate Polymers*, *89*(2), 676–686.

Jouki, M., Mortazavi, S. A., Yazdi, F. T., & Koocheki, A. (2014). Characterization of antioxidant-antibacterial quince seed mucilage films containing thyme essential oil. *Carbohydrate Polymers*, *99*, 537–46.

Juven, B. J., Kanner, J., Schved, F., & Weisslowicz, H. (1994). Factors that interact with the antibacterial action of thyme essential oil and its active constituents. *Journal of Applied Bacteriology*, *76*(6), 626–631.

Kaya, S., & Kaya, A. (2000). Microwave drying effects on properties of whey protein isolate edible films. *Journal of Food Engineering*, *43*(2), 91–96.

Kim, S. O., Ha, T. V. A., Choi, Y. J., & Ko, S. (2014). Optimization of homogenization-evaporation process for lycopene nanoemulsion production and its beverage applications. *Journal of Food Science*, *79*(8), N1604–10.

Kralova, I., & Sjöblom, J. (2009). Surfactants used in food industry: a review. *Journal of Dispersion Science and Technology*, *30*(9), 1363–1383.

Kristo, E., Koutsoumanis, K. P., & Biliaderis, C. G. (2008). Thermal, mechanical and water vapor barrier properties of sodium caseinate films containing antimicrobials and their inhibitory action on Listeria monocytogenes. *Food Hydrocolloids*, *22*(3), 373–386.

Krochta, J. M., Baldwin, E., & Nisperos-Carriedo, M. (1994). *Edible Coatings and Films to Improve Food Quality*. (J. Krochta, E. Baldwin, & M. Nisperos-Carriedo, Eds.). Lancaster, PA: Technomic.

Lagoueyte, N., & Paquin, P. (1998). Effects of microfluidization on the functional properties of xanthan gum. *Food Hydrocolloids*, *12*(3), 365–371.

671 Lambert, R. J. W., Skandamis, P. N., Coote, P. J., & Nychas, G.-J. E. (2001). A study of the
672 minimum inhibitory concentration and mode of action of oregano essential oil, thymol
673 and carvacrol. *Journal of Applied Microbiology*, *91*(3), 453–462.

674 Liang, R., Xu, S., Shoemaker, C. F., Li, Y., Zhong, F., & Huang, Q. (2012). Physical and
675 Antimicrobial Properties of Peppermint Oil Nanoemulsions. *Journal of Agricultural and*
676 *Food Chemistry*, *60*(30), 7548–7555.

677 Ma, X., Chang, P. R., & Yu, J. (2008). Properties of biodegradable thermoplastic pea
678 starch/carboxymethyl cellulose and pea starch/microcrystalline cellulose composites.
679 *Carbohydrate Polymers*, *72*(3), 369–375.

680 Maizura, M., Fazilah, A., Norziah, M. H., & Karim, A. A. (2007). Antibacterial activity and
681 mechanical properties of partially hydrolyzed sago starch-alginate edible film containing
682 lemongrass oil. *Journal of Food Science*, *72*(6), C324–30.

683 McClements, D. J. (2005). *Food Emulsions. Principles, Practices, and Techniques*. (C. Press,
684 Ed.) (p. 609). Boca ratón, FL.

685 McClements, D. J. (2011). Edible nanoemulsions: Fabrication, properties, and functional
686 performance. *Soft Matter*, *7*(6), 2297–2316.

687 McClements, D. J., & Rao, J. (2011). Food-grade nanoemulsions: formulation, fabrication,
688 properties, performance, biological fate, and potential toxicity. *Critical Reviews in Food*
689 *Science and Nutrition*, *51*(4), 285–330.

690 Norajit, K., Kim, K. M., & Ryu, G. H. (2010). Comparative studies on the characterization and
691 antioxidant properties of biodegradable alginate films containing ginseng extract. *Journal*
692 *of Food Engineering*, *98*(3), 377–384.

693 Nuchuchua, O., Sakulku, U., Uawongyart, N., Puttipipatkhachorn, S., Soottitantawat, A., &
694 Ruktanonchai, U. (2009). In vitro characterization and mosquito (Aedes aegypti) repellent
695 activity of essential-oils-loaded nanoemulsions. *AAPS PharmSciTech*, *10*(4), 1234–42.

696 Oriani, V. B., Molina, G., Chiumarelli, M., Pastore, G. M., & Hubinger, M. D. (2014).
697 Properties of cassava starch-based edible coating containing essential oils. *Journal of*
698 *Food Science*, *79*(2), E189–94.

699 Otoni, C. G., Moura, M. R. de, Aouada, F. A., Camilloto, G. P., Cruz, R. S., Lorevice, M. V.,
700 … Mattoso, L. H. C. (2014). Antimicrobial and physical-mechanical properties of
701 pectin/papaya puree/cinnamaldehyde nanoemulsion edible composite films. *Food*
702 *Hydrocolloids*, *41*, 188–194.

703 Otoni, C. G., Pontes, S. F. O., Medeiros, E. A. A., & Soares, N. de F. F. (2014). Edible films
704 from methylcellulose and nanoemulsions of clove bud (Syzygium aromaticum) and
705 oregano (Origanum vulgare) essential oils as shelf life extenders for sliced bread. *Journal*
706 *of Agricultural and Food Chemistry*, *62*(22), 5214–9.

Pérez-Gago, M. B., & Krochta, J. M. (2001). Lipid particle size effect on water vapor permeability and mechanical properties of whey protein/beeswax emulsion films. *Journal of Agricultural and Food Chemistry*, *49*(2), 996–1002.

Pires, C., Ramos, C., Teixeira, B., Batista, I., Nunes, L., & Marques, A. (2013). Hake proteins edible films incorporated with essential oils: Physical, mechanical, antioxidant and antibacterial properties. *Food Hydrocolloids*, *30*(1), 224–231.

Pranoto, Y., Salokhe, V. M., & Rakshit, S. K. (2005). Physical and antibacterial properties of alginate-based edible film incorporated with garlic oil. *Food Research International*, *38*(3), 267–272.

Qian, C., & McClements, D. J. (2011). Formation of nanoemulsions stabilized by model food-grade emulsifiers using high-pressure homogenization: Factors affecting particle size. *Food Hydrocolloids*, *25*(5), 1000–1008.

Rao, J., & McClements, D. J. (2012a). Food-grade microemulsions and nanoemulsions: Role of oil phase composition on formation and stability. *Food Hydrocolloids*, *29*(2), 326–334.

Rao, J., & McClements, D. J. (2012b). Impact of lemon oil composition on formation and stability of model food and beverage emulsions. *Food Chemistry*, *134*(2), 749–57.

Raybaudi-Massilia, R. M., Mosqueda-Melgar, J., & Martin-Belloso, O. (2008). Edible alginate-based coating as carrier of antimicrobials to improve shelf-life and safety of fresh-cut melon. *International Journal of Food Microbiology*, *121*(3), 313–327.

Rojas-Graü, M. A., Avena-Bustillos, R. J., Friedman, M., Henika, P. R., Martin-Belloso, O., & McHugh, T. H. (2006). Mechanical, barrier, and antimicrobial properties of apple puree edible films containing plant essential oils. *Journal of Agricultural and Food Chemistry*, *54*(24), 9262–7.

Rojas-Graü, M. A., Avena-Bustillos, R. J., Olsen, C., Friedman, M., Henika, P. R., Martin-Belloso, O., McHugh, T. H. (2007). Effects of plant essential oils and oil compounds on mechanical, barrier and antimicrobial properties of alginate-apple puree edible films. *Journal of Food Engineering*, *81*(3), 634–641.

Salvia-Trujillo, L., Rojas-Graü, M. A., Soliva-Fortuny, R., & Martín-Belloso, O. (2013). Effect of processing parameters on physicochemical characteristics of microfluidized lemongrass essential oil-alginate nanoemulsions. *Food Hydrocolloids*, *30*(1), 401–407.

Sánchez-González, L., Cháfer, M., Hernández, M., Chiralt, A., & González-Martínez, C. (2011). Antimicrobial activity of polysaccharide films containing essential oils. *Food Control*, *22*(8), 1302–1310.

Sánchez-González, L., Chiralt, A., González-Martínez, C., & Cháfer, M. (2011). Effect of essential oils on properties of film forming emulsions and films based on hydroxypropylmethylcellulose and chitosan. *Journal of Food Engineering*, *105*(2), 246–253.

744 Severino, R., Ferrari, G., Vu, K. D., Donsì, F., Salmieri, S., & Lacroix, M. (2015).
745 Antimicrobial effects of modified chitosan based coating containing nanoemulsion of
746 essential oils, modified atmosphere packaging and gamma irradiation against Escherichia
747 coli O157:H7 and Salmonella Typhimurium on green beans. *Food Control*, *50*, 215–222.

748 Shirazi, M. H., Ranjbar, R., Eshraghi, S., Amin, G., Nouri, M. S., & Bazzaz, N. (2008).
749 Inhibitory Effects of Sage Extract on the Growth of Enteric Bacteria. *Pakistan Journal of*
750 *Biological Sciences*, *11*(3), 487–489.

751 Shojaee-Aliabadi, S., Hosseini, H., Mohammadifar, M. A., Mohammadi, A., Ghasemlou, M.,
752 Hosseini, S. M., & Khaksar, R. (2014). Characterization of κ-carrageenan films
753 incorporated plant essential oils with improved antimicrobial activity. *Carbohydrate*
754 *Polymers*, *101*, 582–91.

755 Solans, C., Izquierdo, P., Nolla, J., Azemar, N., & Garcia-Celma, M. J. (2005). Nano-
756 emulsions. *Current Opinion in Colloid and Interface Science*, *10*(3-4), 102–110.

757 Stang, M., Karbstein, H., & Schubert, H. (1994). Adsorption kinetics of emulsifiers at oil—
758 water interfaces and their effect on mechanical emulsification. *Chemical Engineering and*
759 *Processing: Process Intensification*, *33*(5), 307–311.

760 Ultee, A., Bennik, M. H. J., & Moezelaar, R. (2002). The phenolic hydroxyl group of carvacrol
761 is essential for action against the food-borne pathogen Bacillus cereus. *Applied and*
762 *Environmental Microbiology*, *68*(4), 1561–1568.

763 Vargas, M., Cháfer, M., Albors, A., Chiralt, A., & González-Martínez, C. (2008).
764 Physicochemical and sensory characteristics of yoghurt produced from mixtures of cows'
765 and goats' milk. *International Dairy Journal*, *18*(12), 1146–1152.

766 Vargas, M., Perdones, Á., Chiralt, A., Cháfer, M., & González-Martínez, C. (2011). Effect of
767 homogenization conditions on physicochemical properties of chitosan-based film-
768 forming dispersions and films. *Food Hydrocolloids*, *25*(5), 1158–1164.

769 Ziani, K., Fang, Y., & McClements, D. J. (2012). Fabrication and stability of colloidal delivery
770 systems for flavor oils: Effect of composition and storage conditions. *Food Research*
771 *International*, *46*(1), 209–216.

772 Zúñiga, R. N., Skurtys, O., Osorio, F., Aguilera, J. M., & Pedreschi, F. (2012). Physical
773 properties of emulsion-based hydroxypropyl methylcellulose films: effect of their
774 microstructure. *Carbohydrate Polymers*, *90*(2), 1147–58.

775

7 FIGURE CAPTIONS

Fig. 1. Droplet size distributions expressed in intensity of film-forming EOs-loaded nanoemulsions, (TH-EO: thyme oil; LG-EO: lemongrass oil; SG-EO: sage oil).

Fig. 2. SEM images of the surface of alginate films (ALG) and lemongrass (LG-EO), sage (SG-EO) or thyme (TH-EO) nanoemulsion-based films. (A) Film side dried in contact with air, and (B) film side dried in contact with Mylar paper.

Fig. 3. (A) Tensile strength (TS) and elongation at break (EAB) of alginate films (ALG) and films based on nanoemulsions containing lemongrass (LG-EO), sage (SG-EO) and thyme (TH-EO) oils. (B) Puncture force (PF) of edible films. Error bars indicate standard deviations. Means with the same letter are not significantly different at $p < 0.05$.

Fig. 4. Antimicrobial activity of alginate films containing EOs against *Escherichia coli* inoculated on TSA-NaCl plates. Data shown are a mean ± standard deviation. ▲ CT: Control without film; ■ ALG: alginate films; ● TH-EO: thyme essential oil film; ◆ SG-EO: sage essential oil film and ▪ LG-EO: lemongrass essential oil film.

8 TABLE CAPTIONS

Table 1. Physicochemical characterization of the film-forming nanoemulsions loaded with different EOs. TH-EO: thyme oil; LG-EO: lemongrass oil; SG-EO: sage oil. Z-average is the mean diameter droplet size, PDI refers to polydispersity index, WI is the whiteness index. Values were given as mean ± standard deviations. $^{a.b,c}$ mean values with same superscript within a column are not significantly different ($p < 0.05$).

Table 2. L^*, a^*, b^* values, color difference (ΔE^*) and opacity of alginate films and films made from EO nanoemulsions. ALG: alginate films; TH-EO: thyme essential oil films; SG-

EO: sage essential oil films; LG-EO: lemongrass essential oil films. Data reported are mean values ± standard deviations. [a,b,c] values with the same superscript letters in the same column are not significantly different ($p < 0.05$).

Table 3. Water vapor permeability (WVP) and thickness of alginate films and films made from EO-loaded nanoemulsions. ALG: alginate films; TH-EO: thyme essential oil films; LG-EO: lemongrass essential oil films; SG-EO: sage essential oil films. Values were given as mean ± standard deviations. [a,b,c] Values with the same superscript letters within a column are not significantly different ($p<0.05$).

Table 4. Pearson's correlation coefficients (p-value) between the physical properties of nanoemulsions containing EO and the physical and mechanical properties of their respective edible films.

Table 1. Physicochemical characterization of the film-forming nanoemulsions loaded with different EOs.

Nanoemulsion	Z-average (nm)	PDI	ζ- potential (mV)	WI	Viscosity (mPa.s)
TH-EO	82 ± 3b	0.563 ± 0.024a	-44 ± 6a	27.95 ± 0.06a	452 ± 43a
LG-EO	41 ± 9a	0.52 ± 0.05a	-41 ± 3a	25.38 ± 0.14b	616 ± 62b
SG-EO	35 ± 7a	0.65 ± 0.04b	-70 ± 9b	23.53 ± 0.10c	473 ± 19a

TH-EO: thyme oil; LG-EO: lemongrass oil; SG-EO: sage oil. Z-average is the mean diameter droplet size, PDI refers to polydispersity index, WI is the whiteness index. Values were given as mean ± standard deviations. a.b,c mean values with same superscript within a column are not significantly different ($p < 0.05$).

Table 2. *L**, *a**, *b** values, color difference (*ΔE**) and opacity of alginate films and films made from EO nanoemulsions.

Film	*L**	*a**	*b**	Δ*E**	Opacity
ALG	89.61 ± 0.17^{a}	-0.47 ± 0.03^{b}	4.4 ± 0.4^{a}	24 ± 4^{a}	6.7 ± 0.4^{ab}
TH-EO	88.54 ± 0.25^{b}	-0.83 ± 0.05^{a}	6.9 ± 0.6^{b}	58 ± 9^{b}	7.4 ± 0.5^{b}
LG-EO	93.19 ± 0.19^{c}	-0.47 ± 0.12^{bc}	2.5 ± 0.4^{c}	13 ± 3^{c}	9.7 ± 1.9^{c}
SG-EO	92.72 ± 0.16^{d}	-0.42 ± 0.03^{c}	2.6 ± 0.3^{c}	11.9 ± 1.4^{c}	5.69 ± 0.25^{a}

ALG: alginate films; TH-EO: thyme essential oil films; SG-EO: sage essential oil films; LG-EO: lemongrass essential oil films. Data reported are mean values ± standard deviations. a,b,c values with the same superscript letters in the same column are not significantly different ($p < 0.05$).

Table 3. Water vapor permeability (WVP) and thickness of alginate films and films made from EO-loaded nanoemulsions.

Film	WVP (g/m.s.Pa) $x10^{-10}$	Thickness (µm)
ALG	2.36 ± 0.21^{a}	50 ± 3^{a}
TH-EO	2.18 ± 0.23^{ab}	46 ± 5^{a}
LG-EO	2.12 ± 0.24^{ab}	42 ± 5^{b}
SG-EO	1.9 ± 0.4^{b}	38 ± 3^{b}

ALG: alginate films; TH-EO: thyme essential oil films; LG-EO: lemongrass essential oil films; SG-EO: sage essential oil films. Values were given as mean ± standard deviations. a,b,c Values with the same superscript letters within a column are not significantly different ($p<0.05$).

Table 4. Pearson's correlation coefficients (p-value) between the physical properties of nanoemulsions containing EO and the physical and mechanical properties of their respective edible films.

		PHYSICAL PROPERTIES OF FILM-FORMING NANOEMULSIONS			
		Droplet size	**ζ-potential**	**Whiteness index**	**Viscosity**
PHYSICAL AND MECHANICAL PROPERTIES OF EDIBLE FILMS	**ΔE**	0.9424**	0.4377	0.9128**	-0.5198
		(0.0000)	(0.0900)	(0.0006)	(0.1515)
	Opacity	0.6846	0.7008**	0.2345	0.6159
		(0.8013)	(0.0025)	(0.5437)	(0.0774)
	WVP	0.3945	-0.1434	0.0282	0.2152
		(0.1305)	(0.5962)	(0.9425)	(0.5782)
	Thickness	0.6919**	0.2595	0.6332	-0.2852
		(0.0030)	(0.3319)	(0.0672)	(0.4569)
	Tensile Strength	-0.3389	0.2372	0.1306	0.4582
		(0.1991)	(0.3765)	(0.7377)	(0.2149)
	Elongation at break	-0.5383**	-0.8527**	-0.6317	-0.4449
		(0.0315)	(0.0000)	(0.0680)	(0.2302)
	Puncture Force	0.4233	0.1925	0.5019	0.1177
		(0.1023)	(0.4751)	(0.1686)	(0.7630)

** $p < 0.05$

Fig. 1. Droplet size distributions expressed in intensity of film-forming EOs-loaded nanoemulsions, (TH-EO: thyme oil; LG-EO: lemongrass oil; SG-EO: sage oil).

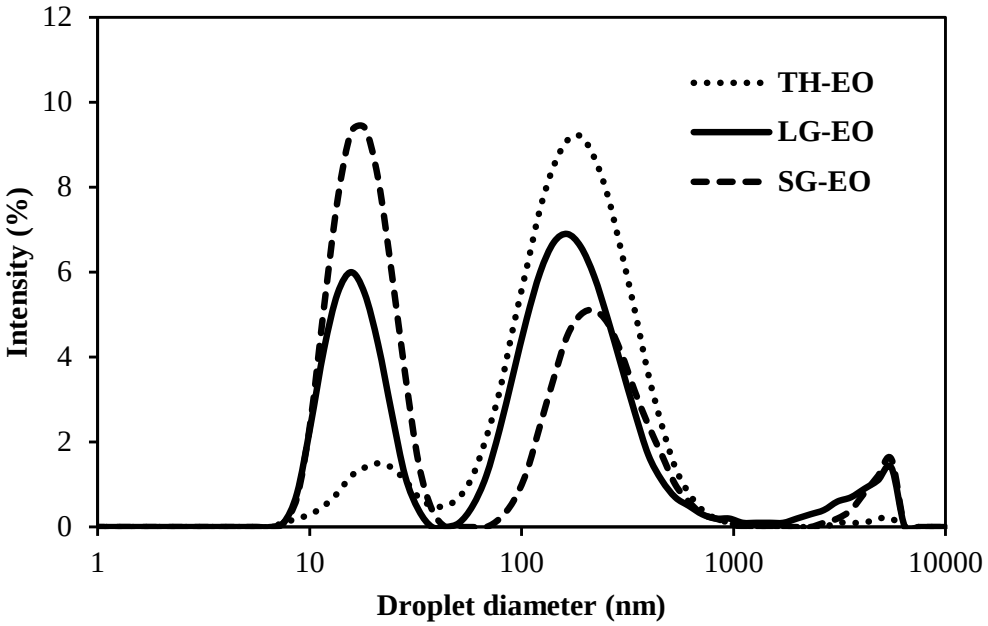

Fig. 2. SEM images of the surface of alginate films (ALG) and lemongrass (LG-EO), sage (SG-EO) or thyme (TH-EO) nanoemulsion-based films.

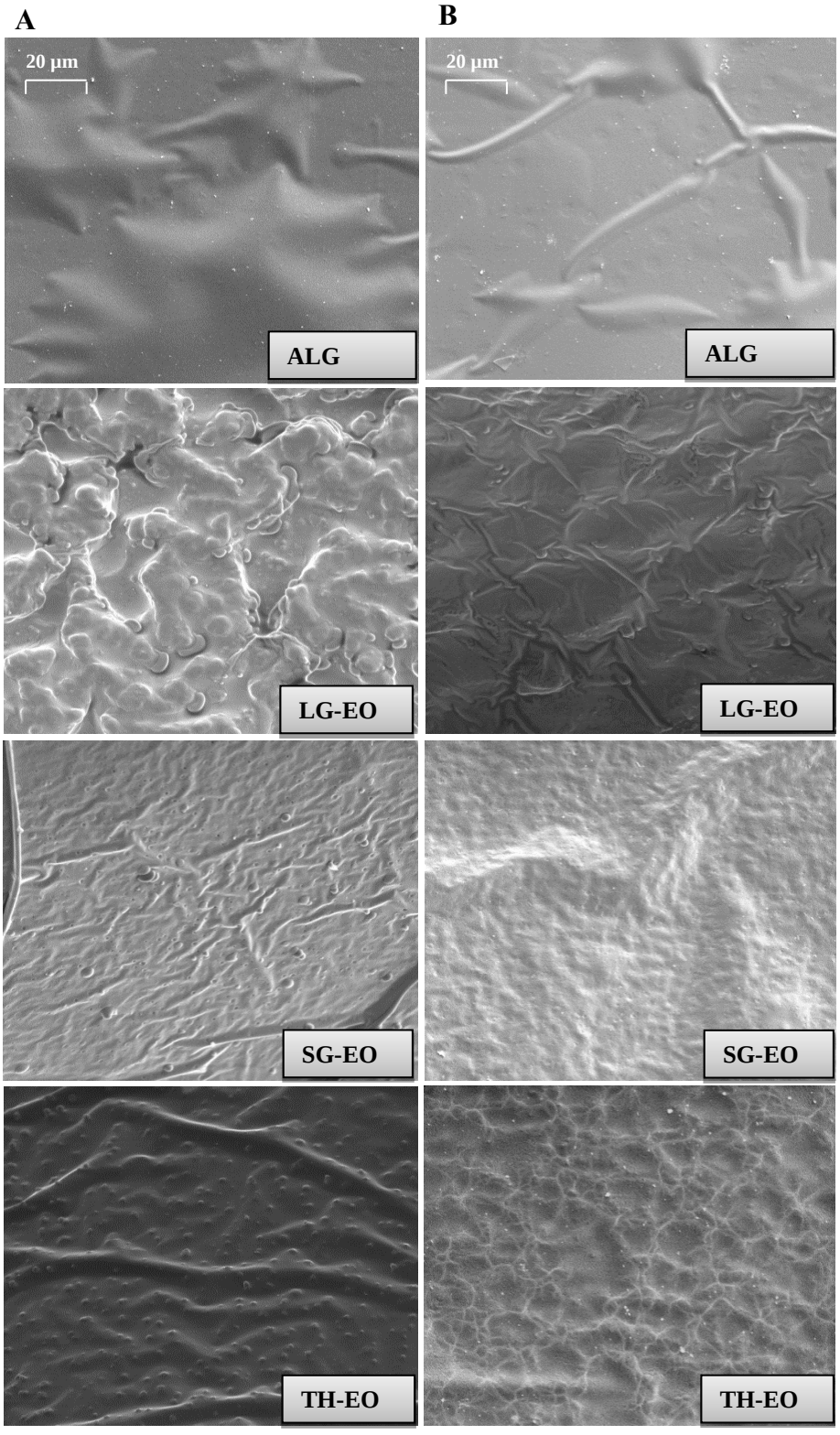

(A) Film side dried in contact with air, and (B) film side dried in contact with Mylar paper.

Fig. 3. (A) Tensile strength (TS) and elongation at break (EAB) of alginate films (ALG) and films based on nanoemulsions containing lemongrass (LG-EO), sage (SG-EO) and thyme (TH-EO) oils. (B) Puncture force (PF) of edible films.

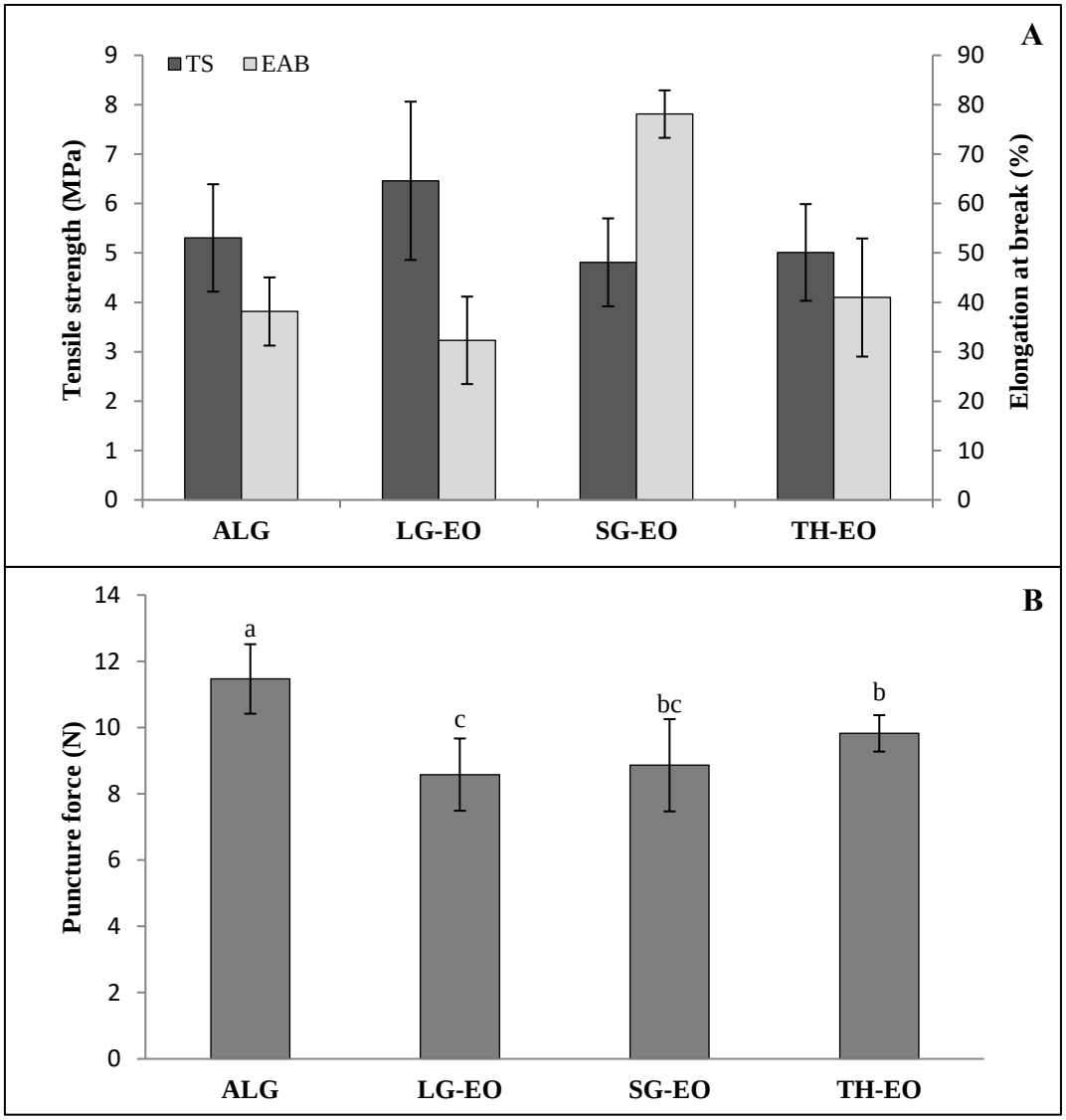

Error bars indicate standard deviations. Means with the same letter are not significantly different at $p < 0.05$

Fig. 4. Antimicrobial activity of alginate films containing EOs against *Escherichia coli* inoculated on TSA-NaCl plates.

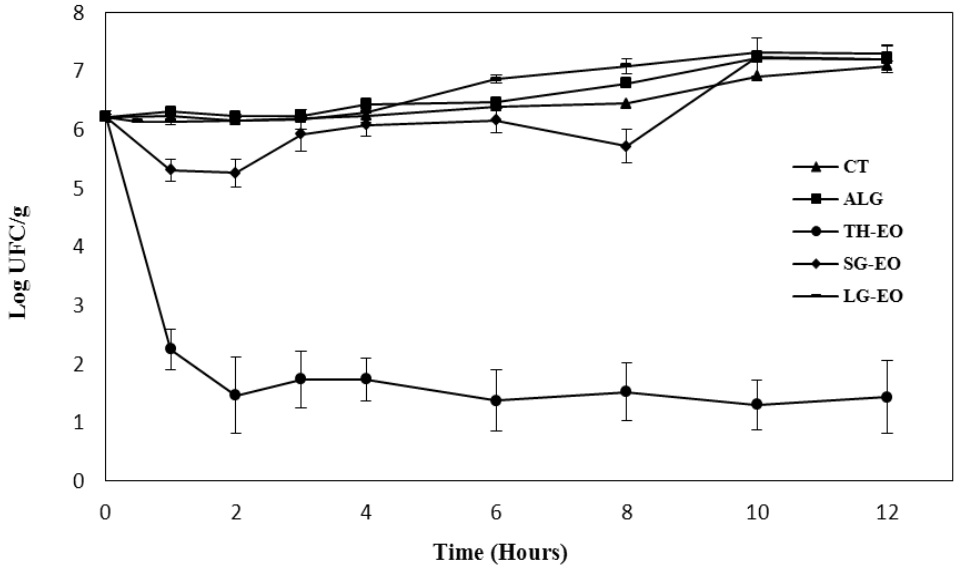

Data shown are a mean ± standard deviation. ▲ CT: Control without film; ■ ALG: alginate films; ● TH-EO: thyme essential oil film; ◆ SG-EO: sage essential oil film and ▪ LG-EO: lemongrass essential oil film.